Geophysical Research Letters

RESEARCH LETTER
10.1029/2019GL086843

Key Points:
- Data assimilation is a skillful technique for reconstructing Arctic sea-ice extent during the satellite era
- Reconstructed sea ice shows large declines in total Arctic sea-ice extent during the early 20th-century warming (1910–1940)
- Trends in total Arctic sea-ice extent during the satellite era are ∼33–38% greater than during the early 20th-century warming

Supporting Information:
- Supporting Information S1

Correspondence to:
M. K. Brennan,
mkb22@uw.edu

Citation:
Brennan, M. K., Hakim, G. J., & Blanchard-Wrigglesworth, E. (2020). Arctic sea-ice variability during the instrumental era. *Geophysical Research Letters*, *47*, e2019GL086843. https://doi.org/10.1029/2019GL086843

Received 24 DEC 2019
Accepted 7 MAR 2020
Accepted article online 13 MAR 2020

©2020. American Geophysical Union. All Rights Reserved.

Arctic Sea-Ice Variability During the Instrumental Era

M. Kathleen Brennan[1], Gregory J. Hakim[1], and Edward Blanchard-Wrigglesworth[1]

[1]Department of Atmospheric Sciences, University of Washington, Seattle, WA, USA

Abstract Arctic sea-ice extent (SIE) has declined drastically in recent decades, yet its evolution prior to the satellite era is highly uncertain. Studies using SIE observations find little variability prior to the 1970s; however, these reconstructions are based on limited data, especially prior to the 1950s. We use ensemble Kalman filter data assimilation of surface air temperature observations with Last Millennium climate model simulations to create a fully gridded Arctic sea-ice concentration reconstruction from 1850 to 2018 and investigate the evolution of Arctic SIE during this period. We find a decline of $\sim 1.25 \times 10^6$ km^2 during the early 20th-century warming (1910–1940). The 25-year trends during this period are ∼33–38% smaller than the satellite era (1979–2018) but almost twice as large as previous estimates. Additionally, we find that variability of SIE on decadal timescales prior to the satellite era is ∼40% greater than previously estimated.

Plain Language Summary Arctic sea ice is an important part of the climate system, serving as the interface between the ocean–atmosphere system. Arctic sea ice has undergone a rapid decline in recent decades, prompting the question of whether there have been changes of similar magnitude in the past. To answer such questions, a long record of sea ice is necessary, but spatially and temporally complete satellite observations are only available starting in 1979. Previous studies combining sea-ice observations from various sources during the Instrumental Era (1850–2014) found little variability in sea-ice extent prior to the satellite era, but data availability is limited prior to the 1950s. Here, we create an independent estimate of Arctic sea ice from 1850 to 2018 using a data assimilation approach that blends more abundant temperature observations with data from climate models. Our results show substantial loss of sea ice between 1910 and 1940, with a trend that is about ∼33–38% less than what has been observed in satellite observations. These results reinforce previous findings not only that the current trend is unprecedented in duration since 1850 but also that sea-ice variability prior to 1979 is ∼40% larger than previously estimated.

1. Introduction

Arctic sea ice is one of the most rapidly changing components of the climate system, affecting surface albedo and modulating ocean–atmosphere interaction through surface fluxes. Large declines in sea ice can impact local ecosystems, human communities, and the global climate system (Meier et al., 2014). Documenting and understanding decadal–centennial variability in sea ice is limited by the availability of high-quality observations, which are only spatially and temporally complete during the satellite era (1978 to present, (Fetterer et al., 2017)). Furthermore, given the presence of strong radiative forcing during this period, it is difficult to partition the relative role of natural variability (e.g., Ding et al., 2017; England et al., 2019) and radiative forcing (Notz & Marotzke, 2012) on the rapid Arctic sea ice decline observed in the satellite record. In order to estimate the natural variability of sea ice, a longer record is needed. Here, we introduce a novel method to reconstruct sea ice cover from 1850 to present, using data assimilation (DA), numerical model data, and observations of surface air temperature (SAT).

The longest Arctic sea-ice extent (SIE) observation-based reconstruction combines various sea-ice observation types, ranging from satellite data to shipping records, to extend Arctic sea ice records back to 1850 (Walsh et al., 2017). The Walsh et al. (2017) reconstruction of SIE (hereafter W17SIE) shows little variability before 1970, particularly on decadal to multidecadal timescales. However, the fidelity of this dataset is limited by gaps in observation availability, particularly before 1953 and during winter months (see below and Figure S1 in the supporting information).

Although direct observations of sea ice are limited in space and time, instrumental observations of SAT are much more abundant. Polar, hemispheric, and global mean SAT, both in observations and climate models,

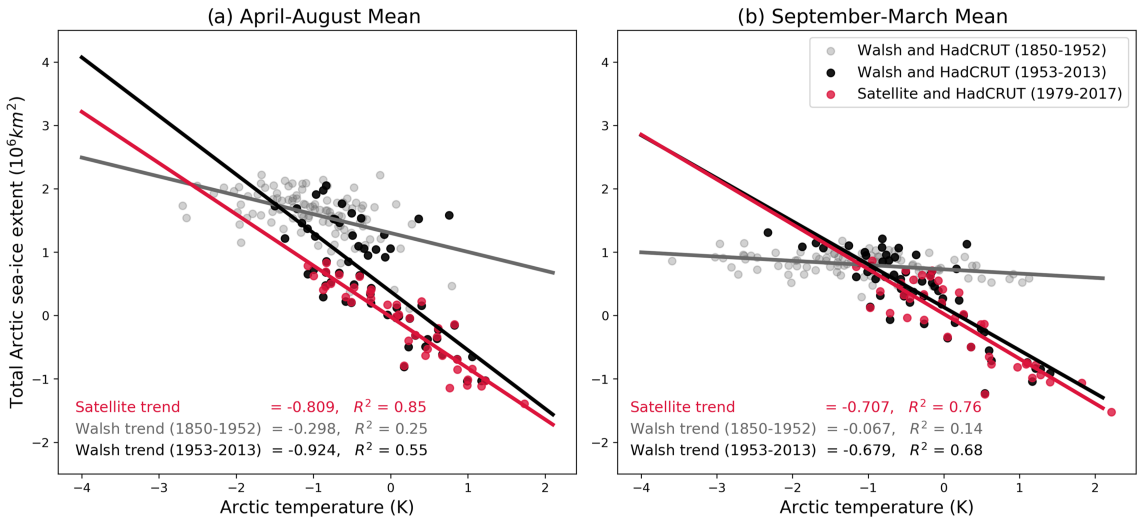

Figure 1. Arctic SAT (averaged north of 65°N, derived from HadCRUT) and total SIE in both the satellite data between 1979 and 2017 (in red) and the Walsh et al. (2017) dataset between 1850–1952 (in gray) and 1953–2013 (in black). Anomalies are relative to 1979–2013.

are known to be tightly coupled to sea-ice variability on annual and longer timescales (e.g., Armour et al., 2011; Gregory et al., 2002; Mahlstein & Knutti, 2012; Olonscheck et al., 2019). Observations show that global mean SAT was relatively stable between 1850 and 1900 (Morice et al., 2012), which may explain low decadal sea-ice variability in W17SIE during this time period. However, during the early 20th century (1900–1940), an anomalous warming event is well documented across Northern Hemisphere high latitudes (e.g., Hegerl et al., 2018). The magnitude of this early 20th-century warming (ETCW) was largest during winter months (Overland et al., 2004; Semenov, 2007) and similar in spatial structure to that observed in the late 20th century.

Despite the SAT anomalies being comparable between the late 20th century and the ETCW, W17SIE shows much less decline during the ETCW than during the late 20th century, with one period of decline of $\sim 0.5 \times 10^6$ km^2 between 1920 and 1945 (see below). The peak loss in W17SIE also lags the period of largest ETCW temperature anomalies seen in observations, which together with the modest decline in SIE would suggest a weak relationship between temperature and sea ice during the ETCW. In this paper, we first investigate the relationship between temperature and sea ice during the Instrumental Era using satellite observations, reanalysis, and W17SIE. Then, we use a DA framework to construct a new independent Arctic sea-ice reconstruction using more abundant SAT observations. We then explore the decline of sea ice during the ETCW in the new reconstruction and compare the ETCW decline to that observed and reconstructed in the satellite era.

2. Temperature and Sea Ice in the Instrumental Era

We analyze the relationship between Arctic SAT derived from the HadCRUT version 4.6.0.0 dataset (HadCRUT, Morice et al., 2012), which uses no infill or interpolation and SIE from W17SIE. Because the observation availability used in W17SIE depends strongly on both season and time period (see section 1 of the supporting information), we partition the analysis into summer and winter seasons (April–August and September–March, respectively) and by time period (pre- and post-1953 for W17SIE, plus the satellite era [1979–2017]). Results show that the relationship between SAT and W17SIE and satellite observations generally agrees during 1953 to present but differs greatly before 1953 (Figure 1).

Specifically, there is a strong linear relationship between SAT and SIE in the satellite record in both seasons as indicated by an R^2 value of 0.76 (September–March) and 0.85 (April–August) in Figure 1. Satellite observations also show slightly stronger sensitivity of SIE–SAT in summer months. W17SIE shows a linear relationship for both seasons between 1953 and 2013, with a similar sensitivity to satellite observations during winter (Figure 1b) and a slightly steeper sensitivity compared to satellite observations during summer

(Figure 1a), but the difference is not statistically different at the 95% confidence level. In contrast, the earlier part of W17SIE, between 1850 and 1952, exhibits a much lower SIE–SAT sensitivity in summer relative to the satellite era (Figure 1a) and almost no SIE–SAT sensitivity in winter (Figure 1b).

There are at least two possible hypotheses for the reduced sensitivity of SIE-SAT in W17SIE before 1953. First, the sensitivity of sea ice may be mean-state dependent, such that in colder, thicker sea-ice regimes (which may have existed in the Arctic during the late 19th and early 20th century) SIE may be less sensitive to changes in temperature. However, model simulations of sea-ice sensitivity to temperature for different mean states (Armour et al., 2011; Mahlstein & Knutti, 2012) do not support this hypothesis. A second hypothesis is that the reduced sensitivity of sea ice to temperature may simply be due to the fact that there are significantly fewer observations available to W17SIE prior to 1953 (see Figure S1). When observations are unavailable, W17SIE relies on spatial and temporal infilling, which could dampen variability. Here, we explore the second hypothesis, which motivates new methods for reconstructing sea ice.

The fidelity of sea-ice reconstructions has broader implications, as they are used for boundary conditions in reanalysis products. The widely used sea surface temperature and sea-ice concentration HadISST2 product (Titchner & Rayner, 2014) incorporates an earlier version of W17SIE (Walsh & Chapman, 2001), which is based largely on temporal and spatial infilling for the first half of the 20th century. Atmospheric reanalysis during the 20th century such as ERA-20C (Poli et al., 2016) commonly uses HadISST2 as a boundary condition. Figure 2 shows temperature trends in ERA-20C and the station-based HadCRUT. While HadCRUT shows large magnitude and spatial extent of SAT trends during the ETCW, in some locations comparable to that during the recent satellite-era warming, ERA-20C shows small trends across the Arctic. The NOAA/CIRES 20th-century reanalysis (Compo et al., 2011) shows even larger biases than ERA-20C (see Figure S2).

We postulate that these atmospheric reanalysis biases during the ETCW are strongly influenced by the small interannual sea-ice variability in the Walsh and Chapman (2001) sea-ice product that serve as boundary conditions. This hypothesis is consistent with Semenov and Latif (2012), who find that the ETCW cannot be simulated with an atmospheric model forced with HadISST1.1 (Rayner, 2003) boundary conditions. Thus, improving sea-ice reconstructions has broad implications, especially for studying high-latitude climate variability.

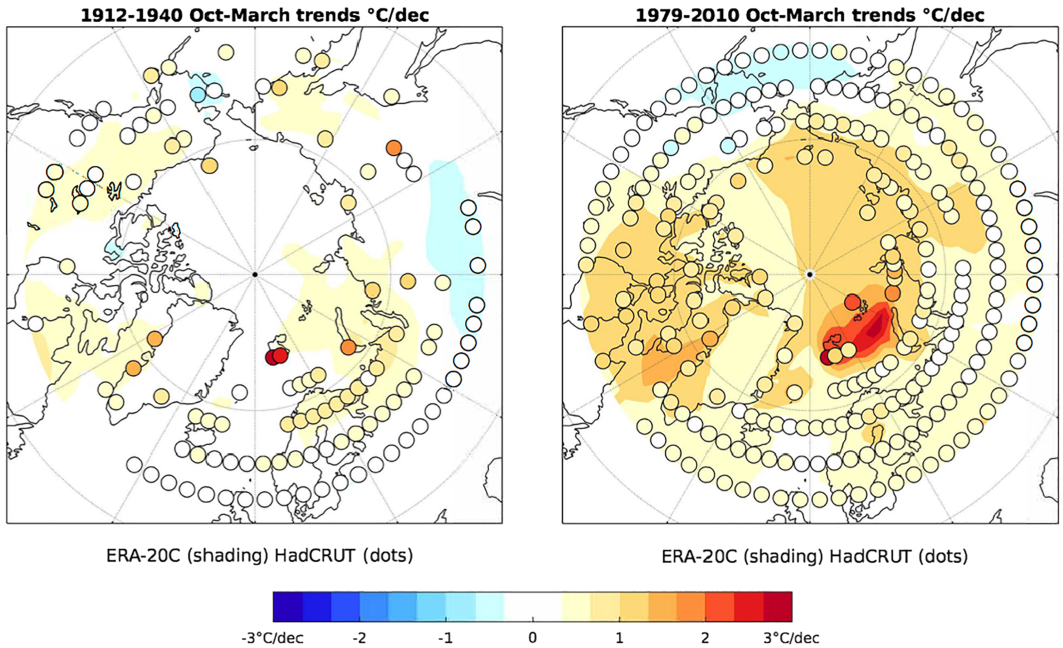

Figure 2. Temperature trends from ERA-20C are shown in shading and that from HadCRUT overlaid as shaded dots for both the early 20th century (1912–1940, left) and satellite era (1979–2010, right).

To this end, we exploit the approximately linear relationship between SAT and Arctic SIE evident in Figure 1 and in the literature (e.g., Mahlstein & Knutti, 2012) and the fact that SAT is the primary driver of sea-ice variability (Olonscheck et al., 2019) to reconstruct sea ice using a DA approach. Other approaches have exploited this relationship to reconstruct sea ice in the 20th century using linear regression models. For example, Connolly et al. (2017) use presatellite temperature trends to recalibrate sea-ice data sources from three regions in the Arctic and find that sea ice retreated after the 1910s and advanced after the mid-1940s, though the magnitude of these changes is relatively small compared to the satellite era. Alekseev et al. (2016) use the relationship between summer SAT and SIE to reconstruct total summer Arctic SIE with a linear regression model, finding a decline of about half that of the recent event (up to 2012) with a minimum extent in 1936, followed by a recovery that peaked around 1970. The main benefit of the DA approach described here is the use of high-quality 2-m air temperature observations with a robust framework for uncertainty quantification (see section 3). Moreover, the results provide fully gridded, spatially consistent climate fields that can be used as boundary conditions for models and to probe the dynamics associated with sea-ice variability.

3. A New Sea-Ice Reconstruction Using Data Assimilation

3.1. Data Assimilation Approach

DA combines information from models with noisy and sparse observations, resulting in a better estimate of climate fields when compared to using models and observations individually. Generally, DA updates a prior estimate, an initial "best guess," of the climate state with new information from observations. DA allows point-wise observations of temperature to influence broader spatial regions of other climate variables, like sea ice, based on the covariance relationships derived from the prior. The weights given to the prior estimate and observations are inversely proportional to their relative uncertainty.

To reconstruct Arctic sea ice, we use an off-line (Oke et al., 2002) ensemble Kalman filter approach to combine Last Millennium climate model simulations (Schmidt et al., 2011; Taylor et al., 2012) with temperature observations. The prior, $\mathbf{x}^b$, is an ensemble of 200 randomly chosen years from these Last Millennium simulations (more details are provided in Section 3.2). The update to this prior estimate derives from the "innovation," which is the difference between annually averaged temperature observations, $\mathbf{y}$, and the prior estimate of these observations $\mathbf{Hx}^b$:

$$\mathbf{x}^a = \mathbf{x}^b + \mathbf{K}(\mathbf{y} - \mathbf{Hx}^b). \tag{1}$$

The innovation weight that results in the analysis, $\boldsymbol{x}^a$, is given by the Kalman gain,

$$\mathbf{K} = \mathbf{B}\,\mathbf{H}^{\mathrm{T}}(\mathbf{HBH}^{\mathrm{T}} + \mathbf{R})^{-1}, \tag{2}$$

where $\mathbf{B}$ is the error covariance matrix of the prior, $\mathbf{R}$ is the error covariance matrix of the observations, and T is the transpose operator. Matrix $\mathbf{H}$ maps the prior to the observations by selecting grid-point data in the prior nearest to the observations. The Kalman gain spreads the new information from temperature observations both spatially and to other climate variables, weighted by the relative uncertainty of each. We sample temperature observations from instrumental data every 10° latitude and longitude, chosen to ensure that the observation errors are uncorrelated and therefore $\boldsymbol{R}$ is diagonal. This assumption allows us to use serial observation processing, which assimilates observations one at a time, simplifying implementation of spatial covariance localization as described below.

To solve (1), we employ a square-root ensemble Kalman filter (Whitaker & Hamill, 2002), which updates the ensemble mean and the perturbations from the ensemble mean separately. The Kalman gain in the update equation for the ensemble perturbations ($\tilde{\mathbf{K}}$) is adjusted by a constant α to yield the correct posterior covariance matrix. Therefore, $\tilde{\mathbf{K}} = \alpha\mathbf{K}$, where, for a single observation, i,

$$\alpha = \left(1 + \sqrt{\frac{\mathbf{R}_{ii}}{\mathbf{HBH}^{T}{}_{ii} + \mathbf{R}_{ii}}}\right)^{-1}, \tag{3}$$

where ii denotes the matrix diagonal entry in the ith row and column.

As is standard practice in ensemble DA, we reduce the effect of spurious long-distance covariances using covariance localization (e.g., Hamill et al., 2001), applying the Gaspari-Cohn fifth-order polynomial function

(Gaspari & Cohn, 1999) with a localization radius (the distance from observations set to zero influence) of 15,000 km.

Kalman filter methods rely on the covariance in the prior ensemble between temperature and the variables of interest (here, sea-ice concentration [SIC]). Climate models tend to underestimate the sensitivity of Arctic sea-ice loss to temperature (Rosenblum & Eisenman, 2017; Stroeve et al., 2007; Winton, 2011). To address this low-sensitivity bias, we inflate the sea-ice perturbations from the prior ensemble means for the simulations used here, MPI and CCSM4 Last Millennium simulations (see Section 3.2), by a factor of 1.8 and 2.6, respectively. The inflation factors are determined empirically by goodness of fit to the observed sea-ice trend during the satellite era. Sensitivity of the results to the localization radius and inflation factor is explored below and in Figures S4 and S5.

Since the Kalman filter method assumes Gaussian distributions and SIC has a range of 0–100%, unphysical values below and above this range are adjusted to 0% and 100%, respectively.

3.2. Data Sources

A 200-member prior ensemble of both SAT and SIC fields is randomly drawn from fully forced Last Millennium model simulations spanning the years 850–1849 CE (Schmidt et al., 2011; Taylor et al., 2012). This ensemble size was chosen because it was computationally inexpensive and revealed small differences in Arctic SIE reconstructions, R^2 >0.97, from tests performed with a 1,000-member prior ensemble. Results using the Community Climate System Model version 4 (CCSM4, Last Millennium simulation, Landrum et al., 2013) and Max Planck Institute for Meteorology (MPI-ESM-P, Last Millennium simulation, Taylor et al., 2012) models are used to determine the sensitivity of the sea-ice reconstructions to climate-model prior and thus the sensitivity of the results to model physics and sea-ice temperature covariance structure. All model output is regridded to a $\sim 2° \times 2°$ grid.

Sensitivity to the choice of instrumental temperature record is tested using three different products: HadCRUT, Berkeley Earth (BE, Rohde et al., 2013), and NASA Goddard Institute for Space Studies (GISTEMP, Hansen et al., 2010). An estimate of the uncertainty in these observations is required when using an ensemble Kalman filter approach (i.e., **R** in equations 2 and 3), and HadCRUT is the only product that provides uncertainty estimates. Various ways of calculating **R** were tested, (see supporting information S1), but in order to use all three products, and for simplicity, we use an uncertainty estimate of 0.4 K^2, which is the area-weighted mean error variance provided by HadCRUT.

4. Arctic Sea-Ice Reconstructions

We first reconstruct annual Arctic SIC from 1850 to 2018 by assimilating HadCRUT SAT with a prior ensemble drawn from the MPI Last Millennium simulation. Figure 3 shows annual Arctic SIE (total area with SIC greater than or equal to 15%) derived from the gridded SIC reconstructions, satellite observations (Fetterer et al., 2017), and W17SIE. The DA-derived time series is the mean of five independent iterations that each use a different 200-member prior ensemble, in order to take into account the uncertainty due to sampling error. Our reconstruction compares well with satellite observations (Figure 3) with an R^2 value of 0.89, detrended R^2 value of 0.43, and coefficient of efficiency (see equation S1) of 0.89 between 1979 and 2017. W17SIE also agrees well with satellite observations, as expected, since it uses satellite data during this time period. The trend during this period is well captured in the reconstructions with a value of $-0.052 \pm 0.012 \times 10^6$ km^2/year compared to -0.055×10^6 km^2/year in satellite observations. Interannual variability is overestimated, with a detrended standard deviation of 0.21×10^6 km^2 in the satellite observations and 0.28×10^6 km^2 in the reconstruction during 1979–2017.

The most notable feature of our reconstruction before the satellite era is the SIE decline during the ETCW, with a total loss of $\sim 1.25 \times 10^6$ km^2 between 1910 and 1940 compared to $\sim 2.0 \times 10^6$ km^2 lost between 1979 and 2017 in satellite observations. Between 1930 and 1950, our reconstruction also shows $\sim 0.5 \times 10^6$ km^2 less SIE than in W17SIE (see Figure 3), and the ETCW minimum occurs approximately 8 years earlier than in W17SIE. Between 1850 and 1900, our reconstruction shows a slow increase in SIE, reaching a maximum just after 1900, as opposed to W17SIE, which shows maximum SIE in the 1960s. Overall, prior to the satellite era, our reconstruction shows greater decadal variability compared to W17SIE, which has relatively constant Arctic SIE between 1850 and 1970. Prior to the satellite era (1850–1979), our reconstruction has a time series standard deviation of 310,000 km^2, whereas W17SIE has standard deviation of 220,000 km^2.

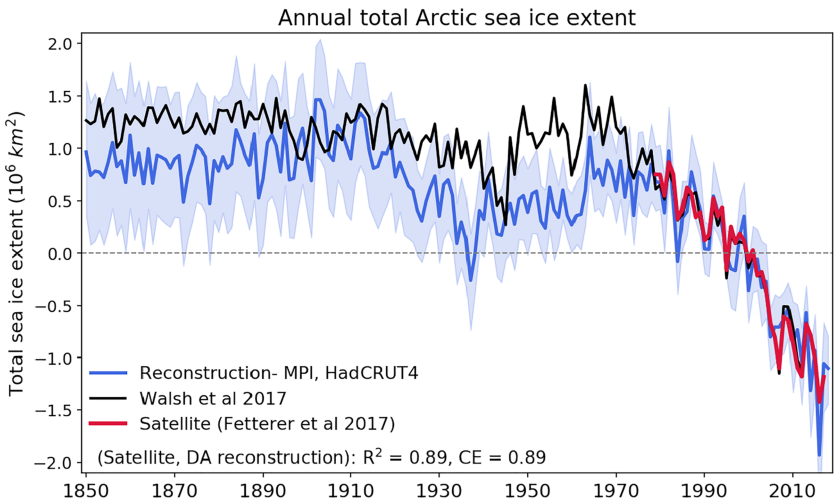

Figure 3. Reconstructed Arctic SIE from DA (blue), Walsh et al. (2017) (black), and satellite observations (red). For our reconstructions, annually averaged HadCRUT temperature data were assimilated with a prior ensemble drawn from the MPI Last Millennium simulation. The blue shaded region indicates the 2.5-97.5th percentile range of reconstructed ensemble members. Anomalies are centered about 1979–2013.

Furthermore, the sensitivity between SIE and SAT in our reconstructions agrees well with that in satellite observations throughout the reconstructed period, whereas W17SIE shows a shift in this sensitivity in the mid-20th century (see Figure S3). We hypothesize that a key source of the discrepancy between our reconstruction and W17SIE generally arises from the limited sea-ice observations available to W17SIE during the earlier portion of the record. When observations are not available, W17SIE relies on spatial and temporal infilling, which could explain the damped variability observed in their reconstructions between 1850 and 1953. Our annual-mean reconstructions generally agree with the summer reconstructions of Arctic SIE in Alekseev et al. (2016), except that their reconstruction shows much larger interannual variability in the early 20th century, and a loss of ~2.0×10^6 km^2 during the 1970s that is not found in our reconstruction.

4.1. Trends and Variability

Here, we compare the magnitude and significance of Arctic SIE trends during the ETCW relative to the satellite era. In our reconstructions, the SIE decline in the ETCW is shorter lived (~25–30 years) than that in the satellite era (~40 years), so we compare the distribution of 25-year trends for both the satellite era and ETCW.

Figure 4 shows the distribution of trends calculated for each ensemble member (from reconstructions using both MPI and CCSM4 model priors) for all possible 25-year segments during the satellite era (1979–2017) and the ETCW (1910–1940). The distribution of all 25-year trends between 1979 and 2017 for both W17SIE and satellite observations is also shown as box plots below the distributions. For W17SIE, ETCW trends were calculated between 1918 and 1948 and are also shown as a box plot (we use a later window for a fair comparison since the minimum SIE occurred 8 years later in W17SIE). The median 25-year trend found in W17SIE during the ETCW of -0.18×10^6 km^2/year falls at the 98th and 99th percentiles of our reconstructions based on the MPI and CCSM4 model priors, respectively. Our reconstructions slightly underestimate the mean 25-year trend in the satellite era. Comparing these two time periods in our reconstructions, the satellite era trends are ~33–38% greater than the ETCW trends.

4.2. Sensitivity of Results

Our reconstruction of SIE depends on the gridded temperature product (and associated errors), the climate model prior, and sample-error mediation in the DA solution (localization length scale and ensemble variance inflation factor). A range of choices for these aspects has been tested, with details provided in the supporting information. Overall, we find that the choice of observational data set and model prior makes little difference to pan-Arctic indices (see Figure S4) but that variance inflation and spatial localization have a larger affect.

With an off-line DA approach, all temporal variability in the reconstruction comes from the observations. Increasing the localization radius and the ensemble variance inflation of sea ice relative to temperature

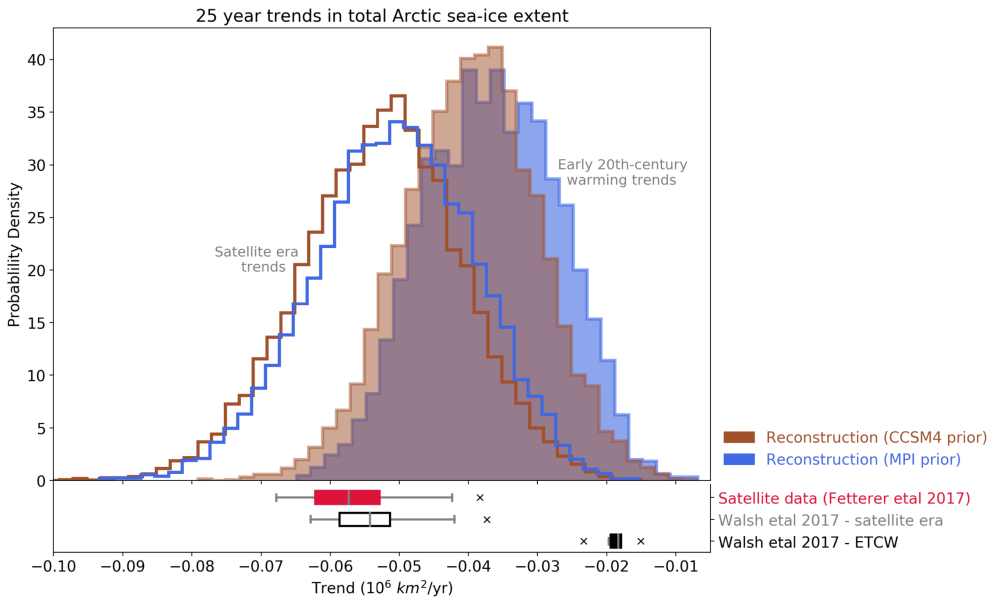

Figure 4. The distribution of all possible 25-year trends in Arctic SIE during the satellite era (1979–2017) and ETCW (1910–1940) for five prior iterations, each containing 200 ensemble members. The probability density functions show reconstructed SIE trends using MPI as the model prior (blue) and CCSM4 (brown). Below the histograms, the spread of trends calculated in W17SIE (black) and satellite observations (red) is displayed as box plots. The ETCW for W17SIE was calculated between 1918 and 1948.

increases the influence of temperature observations, which is realized as larger temporal variability (Figures S5 and S6). The results show a trade-off between capturing decadal variability versus interannual variability. For experiments using the MPI prior and HadCRUT temperature observations, a localization length scale of 15,000 km leads to the best reconstructed trend for nearly all inflation factors, so we chose to use this localization length scale. Given a localization length scale of 15,000 km, the skill metrics are best for an inflation factor of 1.8. For a prior drawn from the CCSM4 Last Millennium simulation and HadCRUT observations, the same localization length scale of 15,000 km was used, and an inflation factor of 2.6 gave the best skill scores. Overall, these experiments show a range of compatible values of localization and ensemble inflation that result in skillful reconstructions relative to satellite observations and similar reconstructions of sea ice for earlier time periods.

5. Conclusions

The relationship between SIE and SAT is approximately linear during the satellite era in observations, but this relationship is much weaker or even absent in W17SIE prior to the 1950s. We speculate that this lower sensitivity of SIE to SAT in W17SIE is due to a lack of high quality sea-ice observations, especially during fall and winter prior to 1953. We also show that 20th-century atmospheric reanalyses underestimate the magnitude of the ETCW (1910–1940) in the Arctic. Since previous versions of W17SIE are used as boundary conditions for 20th-century atmospheric reanalysis, we speculate that the low variability of W17SIE could be a reason atmospheric reanalyses do not fully capture the ETCW, but leave exploration of this hypothesis to future work.

We exploit the relationship between SAT and SIC using an ensemble Kalman filter data assimilation approach to produce a new sea-ice reconstruction. This method combines instrumental temperature observations and model data from Last Millennium simulations to yield skillful Arctic sea-ice reconstructions with annual resolution. Validation against satellite observations yields an R^2 value of 0.89 and coefficient of efficiency of 0.89. Prior to the satellite era, our reconstructions show Arctic SIE loss of ~1.25×10^6 km^2 during the ETCW, which is greater than the ETCW loss of ~$0.75–1.0\times10^6$ km^2 estimated in W17SIE, yet smaller than the SIE loss during the satellite era of ~2.0×10^6 km^2. The average reconstructed 25-year trends of SIE indicate that the rate of sea-ice loss during the ETCW was about ~33–38% smaller than the 25-year trends observed during the satellite era.

Overall, our reconstructions show more interannual variability than in W17SIE during the Instrumental Era with standard deviation ~40% (~90,000 km^2) greater between 1850 and 1979, a significant part of which is due to the ETCW. The ETCW has been ascribed to a combination of anthropogenic forcing and strong natural variability (Beitsch et al., 2014; Delworth, 2000; Fyfe et al., 2013; Wood & Overland, 2009). Here, we find that during the satellite era, Arctic sea-ice loss was larger and longer lasting than during the ETCW, which implies that the current decline likely necessitate external anthropogenic forcing, as previous results have shown (Ding et al., 2017; Kay et al., 2011; Notz & Marotzke, 2012). Future work will extend our data assimilation approach to reconstructing seasonal variability and sea-ice thickness to improve our understanding of sea ice during the Instrumental Era.

Acknowledgments
The authors thank Cecilia Bitz and David Battisti for comments and ideas leading to this project. MKB thanks Luke Parsons for insights into comparing trends and for testing localization and inflation; Robert Tardif for contribution to development of the DA code; Andre Perkins for software debugging help; Jessica Badgeley for productive discussions and support; and Robert Brennan for editing help. MKB was supported by the NSF GRFP program. GH was supported by NSF award AGS-1602223 and NOAA award NA18OAR4310422. EBW was supported by NOAA MAPP grant NA18OAR4310274.

Data Availability Statement

The data for the reconstructions of total Arctic SIE shown here are available online at Zenodo (https://doi.org/10.5281/zenodo.3717240).

References

Alekseev, G., Glok, N., & Smirnov, A. (2016). On assessment of the relationship between changes of sea ice extent and climate in the Arctic. *International Journal of Climatology*, *36*(9), 3407–3412. https://doi.org/10.1002/joc.4550

Armour, K. C., Eisenman, I., Blanchard-Wrigglesworth, E., McCusker, K. E., & Bitz, C. M. (2011). The reversibility of sea ice loss in a state-of-the-art climate model. *Geophysical Research Letters*, *38*, L16705. https://doi.org/10.1029/2011GL048739

Beitsch, A., Jungclaus, J. H., & Zanchettin, D. (2014). Patterns of decadal-scale Arctic warming events in simulated climate. *Climate Dynamics*, *43*(7-8), 1773–1789. https://doi.org/10.1007/s00382-013-2004-5

Compo, G. P., Whitaker, J. S., Sardeshmukh, P. D., Matsui, N., Allan, R. J., Yin, X., et al. (2011). The Twentieth Century Reanalysis Project. *Quarterly Journal of the Royal Meteorological Society*, *137*(654), 1–28. https://doi.org/10.1002/qj.776

Connolly, R., Connolly, M., & Soon, W. (2017). Re-calibration of Arctic sea ice extent datasets using Arctic surface air temperature records. *Hydrological Sciences Journal*, *62*(8), 1317–1340. https://doi.org/10.1080/02626667.2017.1324974

Delworth, T. L. (2000). Simulation of early 20th century global warming. *Science*, *287*(5461), 2246–2250. https://doi.org/10.1126/science.287.5461.2246

Ding, Q., Schweiger, A., L'Heureux, M., Battisti, D. S., Po-Chedley, S., Johnson, N. C., et al. (2017). Influence of high-latitude atmospheric circulation changes on summertime Arctic sea ice. *Nature Climate Change*, *7*(4), 289–295. https://doi.org/10.1038/nclimate3241

England, M., Jahn, A., & Polvani, L. (2019). Nonuniform contribution of internal variability to recent Arctic sea ice loss. *Journal of Climate*, *32*(13), 4039–4053. https://doi.org/10.1175/JCLI-D-18-0864.1

Fetterer, F., Knowles, K., Meier, W. N., Savoie, M., & Windnagel, A. K. (2017). *Sea ice index, version 3*. Boulder, Colorado USA: NSIDC: National Snow and Ice Data Center. https://doi.org/10.7265/N5K072F8

Fyfe, J. C., von Salzen, K., Gillett, N. P., Arora, V. K., Flato, G. M., & McConnell, J. R. (2013). One hundred years of Arctic surface temperature variation due to anthropogenic influence. *Scientific Reports*, *3*(1), 2645. https://doi.org/10.1038/srep02645

Gaspari, G., & Cohn, S. E. (1999). Construction of correlation functions in two and three dimensions. *Quarterly Journal of the Royal Meteorological Society*, *125*(554), 723–757. https://doi.org/10.1256/smsqj.55416

Gregory, J. M., Stott, P. A., Cresswell, D. J., Rayner, N. A., Gordon, C., & Sexton, D. M. H. (2002). Recent and future changes in Arctic sea ice simulated by the HadCM3 AOGCM. *Geophysical Research Letters*, *29*(24), 28–1–28–4. https://doi.org/10.1029/2001GL014575

Hamill, T. M., Whitaker, J. S., & Snyder, C. (2001). Distance-dependent filtering of background error covariance estimates in an ensemble Kalman filter. *Monthly Weather Review*, *129*(11), 2776–2790. https://doi.org/10.1175/1520-0493(2001)129<2776:DDFOBE>2.0.CO;2

Hansen, J., Ruedy, R., Sato, M., & Lo, K. (2010). Global surface temperature change. *Reviews of Geophysics*, *48*, RG4004. https://doi.org/10.1029/2010RG000345

Hegerl, G. C., Brönnimann, S., Schurer, A., & Cowan, T. (2018). The early 20th century warming: Anomalies, causes, and consequences. *Wiley Interdisciplinary Reviews: Climate Change*, *9*(4), e522. https://doi.org/10.1002/wcc.522

Kay, J. E., Holland, M. M., & Jahn, A. (2011). Inter-annual to multi-decadal Arctic sea ice extent trends in a warming world. *Geophysical Research Letters*, *38*, L15708. https://doi.org/10.1029/2011GL048008

Landrum, L., Otto-Bliesner, B. L., Wahl, E. R., Conley, A., Lawrence, P. J., Rosenbloom, N., & Teng, H. (2013). Last millennium climate and its variability in CCSM4. *Journal of Climate*, *26*(4), 1085–1111. https://doi.org/10.1175/JCLI-D-11-00326.1

Mahlstein, I., & Knutti, R. (2012). September Arctic sea ice predicted to disappear near 2°C global warming above present. *Journal of Geophysical Research*, *117*, D06104. https://doi.org/10.1029/2011JD016709

Meier, W. N., Hovelsrud, G. K., van Oort, B. E. H., Key, J. R., Kovacs, K. M., Michel, C., et al. (2014). Arctic sea ice in transformation: A review of recent observed changes and impacts on biology and human activity. *Reviews of Geophysics*, *52*, 185–217. https://doi.org/10.1002/2013RG000431

Morice, C. P., Kennedy, J. J., Rayner, N. A., & Jones, P. D. (2012). Quantifying uncertainties in global and regional temperature change using an ensemble of observational estimates: The HadCRUT4 data set. *Journal of Geophysical Research*, *117*, D08101. https://doi.org/10.1029/2011JD017187

Notz, D., & Marotzke, J. (2012). Observations reveal external driver for Arctic sea-ice retreat. *Geophysical Research Letters*, *39*, L08502. https://doi.org/10.1029/2012GL051094

Oke, P. R., Allen, J. S., Miller, R. N., Egbert, G. D., & Kosro, P. M. (2002). Assimilation of surface velocity data into a primitive equation coastal ocean model. *Journal of Geophysical Research*, *107*(C9), 3122. https://doi.org/10.1029/2000JC000511

Olonscheck, D., Mauritsen, T., & Notz, D. (2019). Arctic sea-ice variability is primarily driven by atmospheric temperature fluctuations. *Nature Geoscience*, *12*(6), 430–434. https://doi.org/10.1038/s41561-019-0363-1

Overland, J. E., Spillane, M. C., Percival, D. B., Wang, M., & Mofjeld, H. O. (2004). Seasonal and regional variation of Pan-Arctic surface air temperature over the instrumental record*. *Journal of Climate*, *17*(17), 3263–3282. https://doi.org/10.1175/1520-0442(2004)017<3263:SARVOP>2.0.CO;2

Poli, P., Hersbach, H., Dee, D. P., Berrisford, P., Simmons, A. J., Vitart, F., et al. (2016). ERA-20C: An atmospheric reanalysis of the twentieth century. *Journal of Climate*, *29*(11), 4083–4097. https://doi.org/10.1175/JCLI-D-15-0556.1

Rayner, N. A. (2003). Global analyses of sea surface temperature, sea ice, and night marine air temperature since the late nineteenth century. *Journal of Geophysical Research*, *108*(D14), 4407. https://doi.org/10.1029/2002JD002670

Rohde, R., Muller, R., Jacobsen, R., Perlmutter, S., & Mosher, S. (2013). Berkeley earth temperature averaging process. *Geoinformatics & Geostatistics: An Overview*, *01*(02), 1–13. https://doi.org/10.4172/2327-4581.1000103

Rosenblum, E., & Eisenman, I. (2017). Sea ice trends in climate models only accurate in runs with biased global warming. *Journal of Climate*, *30*(16), 6265–6278. https://doi.org/10.1175/JCLI-D-16-0455.1

Schmidt, G. A., Jungclaus, J. H., Ammann, C. M., Bard, E., Braconnot, P., Crowley, T. J., et al. (2011). Climate forcing reconstructions for use in PMIP simulations of the last millennium (v1.0). *Geoscientific Model Development*, *4*(1), 33–45. https://doi.org/10.5194/gmd-4-33-2011

Semenov, V. A. (2007). Structure of temperature variability in the high latitudes of the Northern Hemisphere. *Izvestiya - Atmospheric and Ocean Physics*, *43*(6), 687–695. https://doi.org/10.1134/S0001433807060023

Semenov, V. A., & Latif, M. (2012). The early twentieth century warming and winter Arctic sea ice. *The Cryosphere*, *6*(6), 1231–1237. https://doi.org/10.5194/tc-6-1231-2012

Stroeve, J., Holland, M. M., Meier, W., Scambos, T., & Serreze, M. (2007). Arctic sea ice decline: Faster than forecast. *Geophysical Research Letters*, *34*, L09501. https://doi.org/10.1029/2007GL029703

Taylor, K. E., Stouffer, R. J., & Meehl, G. A. (2012). An overview of CMIP5 and the experiment design. *Bulletin of the American Meteorological Society*, *93*, 485–498.

Titchner, H. A., & Rayner, N. A. (2014). The met office Hadley Centre sea ice and sea surface temperature data set, version 2: 1. Sea ice concentrations. *Journal of Geophysical Research: Atmospheres*, *119*(6), 2864–2889. https://doi.org/10.1002/2013JD020316

Walsh, J. E., & Chapman, W. L. (2001). 20th-century sea-ice variations from observational data. *Annals of Glaciology*, *33*(1979), 444–448.

Walsh, J. E., Fetterer, F., Scott Stewart, J., & Chapman, W. L. (2017). A database for depicting Arctic sea ice variations back to 1850. *Geographical Review*, *107*(1), 89–107. https://doi.org/10.1111/j.1931-0846.2016.12195.x

Whitaker, J. S., & Hamill, T. M. (2002). Ensemble data assimilation without perturbed observations. *Monthly Weather Review*, *130*(7), 1913–1924. https://doi.org/10.1175/1520-0493(2002)130<1913:edawpo>2.0.co;2

Winton, M. (2011). Do climate models underestimate the sensitivity of Northern Hemisphere sea ice cover? *Journal of Climate*, *24*(15), 3924–3934. https://doi.org/10.1175/2011JCLI4146.1

Wood, K. R., & Overland, J. E. (2009). Early 20 th century Arctic warming in retrospect. *International Journal of Climatology*, *30*(9), 1269–1279. https://doi.org/10.1002/joc.1973